Inorg. Chem. **2007**, *46*, 586–591

Syntheses and Characterizations of Bismuth Nanofilms and Nanorhombuses by the Structure-Controlling Solventless Method

Jing Chen,[†,‡] Li-Ming Wu,[†] and Ling Chen*[,†]

State Key Laboratory of Structural Chemistry, Fujian Institute of Research on the Structure of Matter, Chinese Academy of Sciences, Fuzhou, Fujian 350002, People's Republic of China, and Graduate School of the Chinese Academy of Sciences, Beijing 100039, People's Republic of China

Received August 9, 2006

Substrate-free bismuth nanofilms with an average thickness of 0.6 nm ($\sigma = \pm 14.1\%$) and monodisperse layered Bi nanorhombuses with an average edge length of 21.5 nm ($\sigma = \pm 14.7\%$) and thickness of 0.9 nm ($\sigma = \pm 25.8\%$) have been successively synthesized by structure-controlling solventless thermolysis from a new layered bismuth thiolate precursor with a 31.49 Å spacing. The morphologies result from self-control at an atomic level by the layered $Bi(SC_{12}H_{25})_3$ crystal structure. The formation of the Bi nanofilm intermediate provides significant substantiation for this synthesis method, and detailed evidence on the conversion progress has been obtained. Both the films and the rhombuses have been characterized by X-ray powder diffraction (XRD), transmission electron microscopy (TEM), energy-dispersive X-ray spectrometry (EDX), high-resolution TEM (HRTEM), and atomic force microscopy (AFM) measurements. Special UV–vis electronic absorption spectra of the nanoproducts have been studied.

Introduction

The booming development of nanoscience and technology has been accelerated by the discoveries of the various special properties associated with the size and shape of the nanomaterials. Well-controlled synthesis is one of the most important factors in nanoscience, especially when applications are concerned, and the greatest challenge is the development of the controlled synthetic methodologies. Numerous chemical approaches have been explored, and some have been proven to be successful in the control of size and morphology of the nanoproduct. Generally, the controlling factors are reactant concentration, solvent, temperature, pressure, and so forth; however, other possible factors are seldom discussed.[1] The solventless method is a newly established chemical approach to nanomaterial synthesis that has successfully generated diverse materials such as sulfides and metals over a wide range of morphologies (wires, belts, rods, fabric, disks, prisms, and spheres).[2−6] We have delineated three important steps in the solventless method: (i) the preparation of a uniform complex/colloidal precursor in solution, (ii) the separation of the precursor from solution, and (iii) the decomposition of the solvent-free precursor under well-defined conditions. The nanoproducts are produced during the third step in which coagulative growth caused by the molecule/particle diffusion is largely reduced under a solventless condition.

Our previous studies on Cu_2S revealed that the uniform nanowires, rods, or spheres could be made from the corresponding precursors obtained from the solutions with different viscosities.[5] The viscosity is considered to be an important indicator of the colloidal precursor polymerization or association. This dependence of nanoproduct morphology

* To whom correspondence should be addressed. E-mail: chenl@fjirsm.ac.cn.
† Fujian Institute of Research on the Structure of Matter.
‡ Graduate School of the Chinese Academy of Sciences.

(1) (a) Cobden, D. H. *Nature* **2001**, *409*, 32−33. (b) Tang, Z.-Y.; Kotov, N. A.; Giersig, M. *Science* **2002**, *297*, 237−240. (c) Volokitin, Y.; Sinzig, J.; deJongh, L. J.; Schmid, G.; Vargaftik, M. N.; Moiseev, I. I. *Nature* **1996**, *384*, 621−623. (d) Xia, Y.-N.; Yang, P.-D.; Sun, Y.-G.; Wu, Y.-Y.; Mayers, B.; Gates, B.; Yin, Y.-D.; Kim, F.; Yan, H.-Q. *Adv. Mater.* **2003**, *15*, 353−389. (e) Lee, G. H.; Huh, S. H.; Jeong, J. W.; Choi, B. J.; Kim, S. H.; Ri, H. C. *J. Am. Chem. Soc.* **2002**, *124*, 12094−12095. (f) Venkatasubramaniam, R.; Siivola, E.; Colpitts, T.; O'Ouinn, B. *Nature* **2001**, *413*, 597−602. (g) Harman, T. C.; Taylor, M. P. J.; Walsh, M. P.; Laforge, B. E. *Science* **2002**, *297*, 2229−2232.

(2) Michael, B.; Sigman, J.; Ghezelbash, A.; Hanrath, T.; Aaron, E.; Saunders, F. L.; Korgel, B. A. *J. Am. Chem. Soc.* **2003**, *125*, 16050−16057.
(3) Ghezelbash, A.; Sigman, M. B.; Korgel, B. A. *Nano Lett.* **2004**, *4*, 537−542.
(4) Sigman, M. B.; Korgel, J.; Korgel, B. A. *Chem. Mater.* **2005**, *17*, 1655−1660.
(5) Chen, L.; Chen, Y.-B.; Wu, L.-M. *J. Am. Chem. Soc.* **2004**, *126*, 16334−16335.
(6) Chen, Y. B.; Chen, L.; Wu, L.-M. *Inorg. Chem.* **2005**, *44*, 9817−9822.

10.1021/ic0615067 CCC: $37.00
Published on Web 12/21/2006

on the precursor state (viscosity) encouraged us to speculate whether a precursor with a selected structure might generate a nanoproduct with a controlled shape. Such speculation was supported by our recent discoveries of the conversion of solid layered precursors to layered silver nanodisks,[6] for which we proposed that the crucial item that determined the layered morphology of the Ag nanodisks was the precursor crystal structure. That is, the initial Ag nuclei concentration and distribution and the consequent atom diffusion paths and speeds are restricted by the precursor crystalline structure. In other words, such a conversion could be regarded as a growth mechanism self-constrained at the atomic level by the precursor structure. Unfortunately, we could not establish additional facts to support such an idea, so a great deal of guessing appeared necessary to describe the conversion of the layered crystalline structure to the layered morphology of an individual nanoparticle. On the other hand, characterization of some intermediate state between the two end materials (the crystalline precursor and the isolated layered nanoproduct) would afford convincing support for our structure-controlling conversion mechanism. In this paper, we report a new example of a layered-precursor to layered-nanoproduct conversion via this solventless method that is significant because a Bi nanofilm intermediate has been obtained.

Bismuth is a semimetal with a small indirect band gap and an anisotropic effective electron mass and could convert to a semiconductor when the size is decreased enough.[7] Many previous efforts have investigated the special properties of Bi nanoparticles, it being thermoelectric for example.[8] Nanoparticles with different morphologies such as wires[10] and tubes[9−11] have been prepared by a variety of methods. In comparison, our Bi nanorhombuses exhibit similar UV−vis absorption behaviors, whereas the nanofilms exhibit unique electronic transitions in the same energy range.

Experimental Section

The reactants were used without any further purification: $C_{12}H_{25}SH$ (Lancaster, 98%), $Bi(NO_3)_3{\cdot}5H_2O$ (A.R., Shanghai Chemical Co.), ethanol (A.R., Shanghai Chemical Co.), chloroform (A.R., Shanghai Chemical Co.), and dimethylformamide (DMF, A.R., Shanghai Chemical Co.).

Synthesis of the Precursor. In a typical procedure, $Bi(NO_3)_3{\cdot}5H_2O$ (2.328 g) was dissolved in 10 mL of DMF, and 2 mL of 1-dodecanethiol (DT, $C_{12}H_{25}SH$) was added with stirring. The yellow precipitate was filtered 30 min later, washed with ethanol, and dried at room temperature. The precursor was determined to be a single-phase layered bismuth dodecanethiolate according to large 0*k*0 spacings in the powder X-ray diffraction (XRD, see details below). In addition, the suggested formula $Bi(SC_{12}H_{25})_3$ was further confirmed by the element analysis on the dried sample. Anal. Calcd: C, 53.18; H, 9.30; N, 0; S, 11.83. Found: C, 53.06; H, 9.09; N, 0.26; S, 11.79.

Syntheses of Bi Nanoproducts. A 0.505 g sample of the yellow precursor was sealed in a glass tubing of 1.3 cm diameter and about 12 cm length which was sealed at a residual pressure < 0.58 Pa. The assembly was subsequently heated in a conventional tube furnace at 90 °C for different times to produce black nanoproducts with different morphologies. For example, a 2 h heating time resulted in Bi nanofilms, and a 5 h heating time resulted in Bi nanorhombuses. The products were usually dispersed in $CHCl_3$ and reprecipitated by the addition of excess ethanol. The yields are about 20% on the basis of $Bi(NO_3)_3{\cdot}5H_2O$.

Characterizations. XRD, transmission electron microscopy (TEM), high-resolution TEM (HRTEM), and atomic force microscopy (AFM) were used to characterize the structure, composition, size, and shape of the synthesized nanoproducts, respectively. The XRD patterns were collected at room temperature with the aid of a D-MAX-2500 diffractometer and Cu Kα radiation. The TEM images were obtained using a JEM 2010 transmission electron microscope equipped with a field emission gun operating at 200 kV. Images were acquired digitally using a Gatan multipole scanning CCD camera with an imaging software system. Energy-dispersive X-ray spectrometry (EDX) analyses of nanoproducts were performed on a carbon-film-coated Cu grid with the aid of a JEM 2010 transmission electron microscope equipped with an Oxford INCA spectrometer. The elemental chemical analyses were performed by Vario EL III (Elementar Co.). The UV−vis spectra were measured on a Perkin-Elmer Lambda-900 spectrophotometer.

Results and Discussion

Layered Crystal Structure of $Bi(SC_{12}H_{25})_3$ Precursor. The organothiolate anion (RS^-) is a fundamental ligand in metal complexes that can be compared with HS^- and S^{2-}. Among the numerous thiolates, the metal ions are usually transition metals, such as Zn^{2+}, Cd^{2+}, Hg^{2+}, Cu^+, Ag^+, Au^{3+}, Fe^{2+}, Co^{3+}, Ni^{2+}, and so forth, or main-group metal ions, for example, Sn^{4+} and Pb^{2+}. Although some bismuth complexes have been postulated, for example, $Bi(SPh)_x(SePh)_{3-x}$ and $Bi[(SC_6F_5)_4]^-$, very few bismuth thiolates have been synthesized and characterized.[12] Herein, we have successfully synthesized a novel bismuth dodecanethiolate, as described above, and have studied its dominant structural motif. Considering the charge balance, we assume the stoichiometry of the precursor to be $Bi^{3+}[(SC_{12}H_{25})^-]_3$, as supported by the elemental analysis results. The powder XRD experiment revealed that the as-synthesized precursor is a pure phase with a layered structure with a large interlayer *d* spacing (Figure 1). The intense narrow reflections of the polycrystalline precursor contain all successive 0*k*0 orders for $k = 2-16$. The measured *kd* values of all 15 reflections fall in the range of 31.46−31.59 Å with an average of 31.49 Å (Supporting Information Table 1), about twice the expected length of the alkyl chain (*L*). Such a layered motif is similar to that of the silver analogue which has a 34.6 Å spacing.[6]

(7) (a) Isaacson, R. T.; Williams, G. A. *Phys. Rev.* **1969**, *185*, 682−688. (b) Black, M. R.; Lin, Y.-M.; Cronin, S. B.; Rabin, O.; Dresselhaus, M. S. *Phys. Rev. B* **2002**, *65*, 195417.

(8) (a) Costa-Krämer, J. L.; García, N.; Olin, H. *Phys. Rev. Lett.* **1997**, *78*, 4990−4993. (b) Black, M. R.; Hagelstein, P. L.; Cronin, S. B.; Lin, Y.-M.; Dresselhaus, M. S. *Phys. Rev. B* **2003**, *68*, 235417. (c) Liu, K.; Chein, L. C. *Appl. Phys. Lett.* **1998**, *73*, 1436−1438.

(9) Wang, Y.-W.; Hong, B.-H.; Kim, K. S. *J. Phys. Chem. B* **2005**, *109*, 7067−7072.

(10) (a) Zhang, Z.-B.; Gekhtman, D.; Dresselhaus, M. S.; Ying, J.-Y. *Chem. Mater.* **1999**, *11*, 1659−1665. (b) Wang, J.-W.; Wang, X.; Peng, Q.; Li, Y.-D. *Inorg. Chem.* **2004**, *43*, 7552−7556.

(11) Li, Y.-D.; Wang, J.-W.; Deng, Z.-X.; Wu, Y.-Y.; Sun, X.-M.; Yu, D.-P.; Yang, P.-D. *J. Am. Chem. Soc.* **2001**, *123*, 9904−9905.

(12) Dance, I. G. *Polyhedron* **1986**, *5*, 1037−1104.

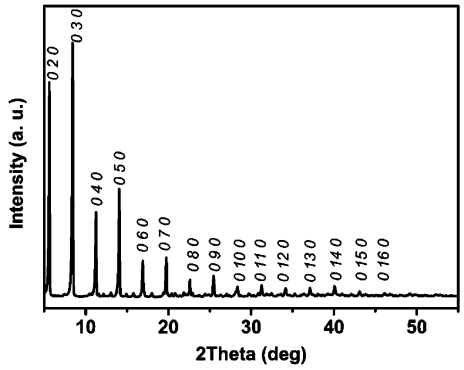

Figure 1. XRD pattern of the $Bi(SC_{12}H_{25})_3$ precursor.

The structure of the as-synthesized $Bi(SC_{12}H_{25})_3$ is also proposed to consist of a central layer of Bi/S with the alkyl chain tails all extending on both sides of the central layer, making the interlayer distance about 2*L*. A difference between the silver and the bismuth salts will originate from different details of the intralayer structure, particularly because the two metals possess a different coordination number (CN) of thiol ligands. That for silver is probably 4, whereas that for bismuth is probably 4, 5, or even 6. A trigonal bipyramid (CN = 5) is probably more likely. The (*h*0*l*) and so forth reflections are all too weak in the powder data to allow for the investigation of the intralayer structural details; on the other hand, the absence of any other non-axial reflections is consistent with a preferred crystallographic registry of layers. Although powder diffraction data give good evidence for the layered motif, the structure needs to be confirmed by single-crystal diffraction studies. However, the common problem for most of the associated metal thiolate polymers, the insolubility of $Bi(SR)_3$, makes it extremely difficult to obtain crystals with a quality sufficient for single-crystal diffraction analysis.

As far as our structure-controlling solventless thermolysis process is concerned, knowing the anisotropic layered nature of the $Bi(SC_{12}H_{25})_3$ precursor already provides enough information for us to understand the conversion process.

Structures and Morphologies of the Bi Nanoproducts. Novel Bi nanofilms free of any substrate have been obtained upon heating the as-synthesized layered $Bi(SC_{12}H_{25})_3$ precursor in a sealed glass tube at 90 °C for 2 h. Similar to the formation of the metallic Ag disks from the Ag(SR) precursor,[6] the Bi^{3+} here is thought to be reduced by the thiolate anion (SR^-) through the electron transfer from the thiolate (SR^-), the two ($SR^\bullet$) radicals yielding the disulfide.[13] It is interesting that when heating is carried out in a N_2 atmosphere up to 150 °C for 2 h, pure Bi is also produced (Supporting Information Figure 1), but at a higher temperature, for example, 250 °C, Bi_2S_3 is formed (Supporting Information Figure 2), which is consistent with the results in the literature.[4] The uniformity of the Bi nanofilm is demonstrated in Figure 2a. This is evidently the first time that thin, uniform, and free-standing bismuth nanofilms have been reported. Such films give no powder XRDs, which indicates that the films are amorphous. Elemental analyses by EDX on several different spots on the film (Figure 2a) consistently reveal only Bi. A typical EDX spectrum recorded on an individual film is shown in Supporting Information Figure 3a. The layered characteristic is obvious in the TEM observation in Figure 2a, which is further confirmed by the AFM analysis shown in Figure 3, in which the thickness of the film is measured to be 0.6 nm ($\sigma = \pm 14.1\%$) (Supporting Information Figure 6). The morphology of the Bi nanofilm is found to be flat and rigid, which is different from the "rag" sheet-like structure of MoS_2.[14] Such differences may come from their different crystallographic structures. The bulk MoS_2 features a hexagonal layered structure in which the motions between the layers are flexible and similar to that in carbon; such flexibility may result in the soft rag-like morphology. Contrarily, the bulk Bi is a three-dimensional rhombohedral network, which may lead to the rigid nanofilm as shown in Figure 2a and Supporting Information Figure 8.

Interestingly, similar treatment of the layered $Bi(SC_{12}H_{25})_3$ precursor at the same temperature but for an elongated time (5 h) generates uniform rhombuses with layered structural motifs (Figure 2b−f). Remarkably, the individual rhombuses are organized in a quasi closed-packed two-dimensional array. A selected area electron diffraction (SAED) investigation of them shows sharp diffraction spots (Figure 2d) and thence their crystalline characteristics. The XRD patterns (Figure 5) of the rhombuses formed in 5 h show sharp intense reflection peaks that can be well-indexed as rhombohedral (ICSD 64705; space group $R\bar{3}m$, 166; $a = b = 4.533(3)$ Å, $c = 11.797(6)$ Å). There is no evidence for a preferred orientation in agreement with the TEM and SAED observations. Compared with the film formed in 2 h, the rhombuses are naturally better crystallized, which is reasonable because of the extended reaction time. The XRD patterns of the rhombuses indicate single-phase bismuth and no other phases. Such singularity is confirmed by the EDX spectrum (Supporting Information Figure 3b). The rhombuses show nice uniformity of shape and size under these conditions, with edge lengths of around 21.5 nm ($\sigma = \pm 14.7\%$) (Figure 2, Supporting Information Figure 5) and the thicknesses of about 0.9 nm ($\sigma = \pm 25.8\%$) according to AFM measurements (Figure 4, Supporting Information Figure 7). The layer motifs are clearly seen in Figure 4 (bottom) as well. The HRTEM image of the single rhombus in Figure 2f shows interplanar distances of 3.25 Å, which correspond to the d_{102} and d_{012} of rhombohedral Bi phase.

UV−Visible Absorption Spectra of the Nanofilms and Nanorhombuses. The UV−vis absorption spectra of the Bi films and rhombuses suspended in $CHCl_3$ (1 mg of Bi in 5 mL of $CHCl_3$) are shown in Figure 6. The rhombuses show a sharp absorption band at approximately 274 nm, in good agreement with the 280 nm absorption for Bi nanoparticles with 13 nm diameters found by Wang et al.[9] The films show two absorption maxima at approximately 257 nm and 362 nm. The former is similar to the 253 nm peak found in an

(13) Oae, S. *Organic Sulfur Chemistry: Structure and Mechanism;* CRC Press: Boca Raton, FL, 1991; Chapter 6, pp 204−206.

(14) Chianelli, R. R.; Prestridge, E. B.; Pecoraro, T. A.; Deneufville, J. P. *Science* **1979**, *203*, 1105−1107.

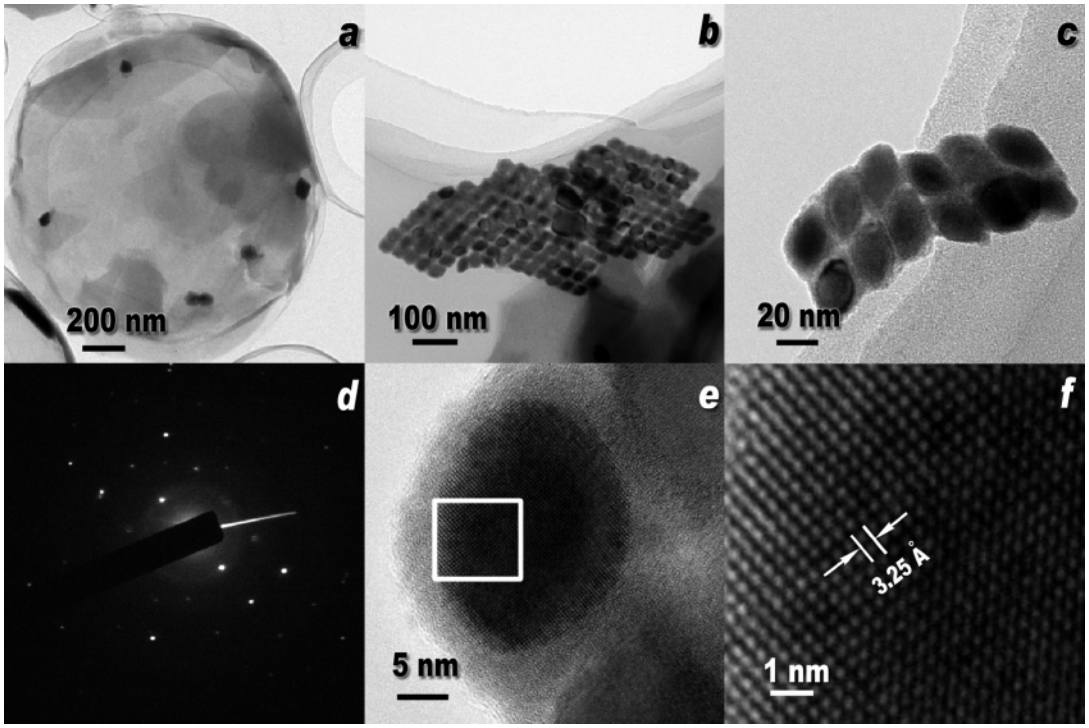

Figure 2. TEM images of Bi nanoparticles: (a) image of nanofilm, (b) low-magnification TEM image of the nanorhombuses monolayer array, (c) high-magnification TEM image of the nanorhombuses, (d) SAED pattern of the nanorhombus from c, (e) corresponding HRTEM image of a single nanorhombus in c, and (f) an enlarged image of the selected part of panel e.

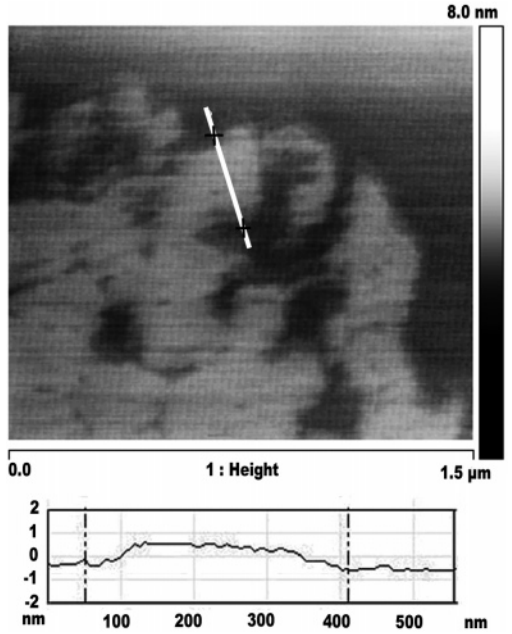

Figure 3. (top) AFM image of a Bi nanofilm produced at 90 °C for 2 h, and (bottom) the height profile along the line in the top figure. The thickness is about 0.6 nm.

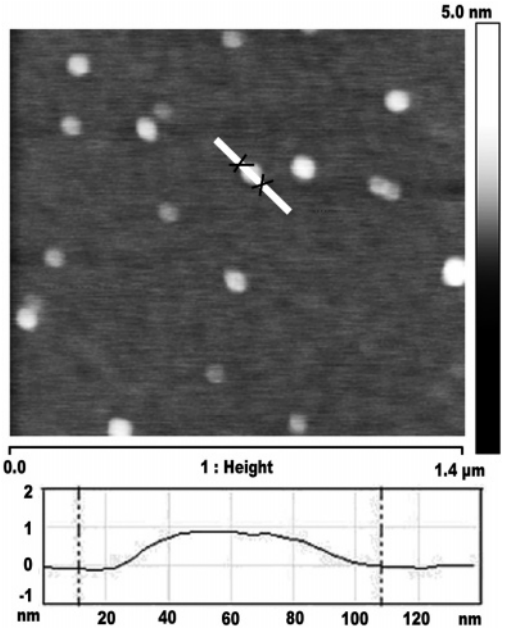

Figure 4. (top) AFM image of the Bi nanorhombuses produced at 90 °C for 5 h, and (bottom) the height profile along the line in the top figure. The height is about 0.9 nm.

aqueous solution of Bi particles with mean diameters of 20 nm by Gutiérrez and Henglein.[15a] The 362 nm absorption has not been reported and might be related to the unique film morphology. The overall trend for both films and rhombuses is an increasing absorption with decreasing wavelength in the 200−800 nm range which is consistent with the theoretical predictions in the usual UV−vis range.[15] The Bi−Bi distance in bulk bismuth is around 3 Å; therefore, a film of 0.6 nm thickness is only two to three atoms thick. The quantum confinement effect in such a film would be significant, and the as-synthesized film might be an ideal candidate for the study of the enhancement of the thermoelectric figure of merit for bismuth.[1f]

Layered Precursor to Layered Nanorhombus: Conversion via an Intermediate Nanofilm. The layered Bi

(15) (a) Gutiérrez, M.; Henglein, A. *J. Phys. Chem.* **1996**, *100*, 7656−7661. (b) Foos, E. E.; Stroud, R. M.; Berry, A. D.; Snow, A. W.; Armistead, J. P. *J. Am. Chem. Soc.* **2000**, *122*, 7114−7115.

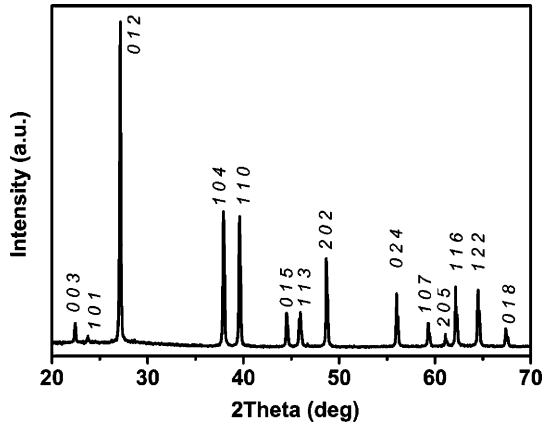

Figure 5. XRD pattern of the nanorhombuses produced at 90 °C in 5 h.

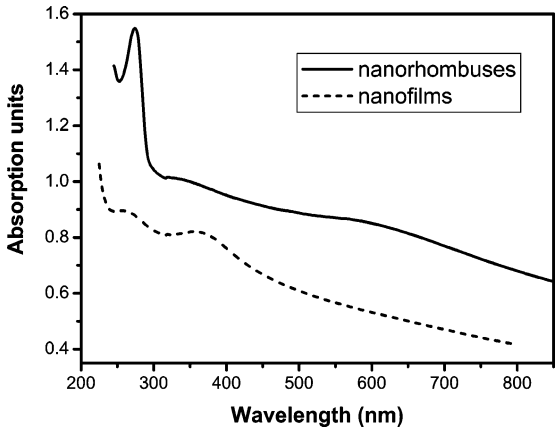

Figure 6. Room-temperature UV−vis absorption spectra of a chloroform suspension of a collection of Bi nanofilms produced at 90 °C for 2 h and nanorhombuses formed at 90 °C over 5 h.

rhombuses have been repeatedly obtained by the thermal decomposition of $Bi(SC_{12}H_{25})_3$ at 90 °C for 5 h (see Figure 2b−f). Such an observation is a good analogue of our previous discovery of the conversion of a layered silver precursor to Ag nanodisks. In order to understand the formation of the present rhombuses, we have explored different annealing times. Annealing at 90 °C for less than 2 h results in a product that retains mainly the precursor. An extension of the duration to 2 h produces a black powder with no XRD pattern, which is pure bismuth and possesses a film morphology (Figure 2a). The XRD patterns of the samples produced in elongated periods of 3, 4, and 5 h are all those of pure rhombohedral bismuth. (Figure 5, Supporting Information Figure 4). The products heated for 3 h are still mostly films, but the X-ray detectable rhombuses appeared also (Figure 7a, Supporting Information Figure 4a). With the time increasing to 4 h, the products are mainly nanorhombuses accreted on the film (Figure 7b, Supporting Information Figure 4b). Pure nanorhombuses are made after being annealed for 5 h. Thus, the formation of the rhombuses takes place in two stages during such a process: the formation of the amorphous film and the crystallization and growth of the rhombuses. At first, $Bi(SC_{12}H_{25})_3$ decomposes to bismuth atoms in a distribution that inherits the layered pattern of the mother structure, and amorphous films are formed during which the long-chain alkyl ligands play an

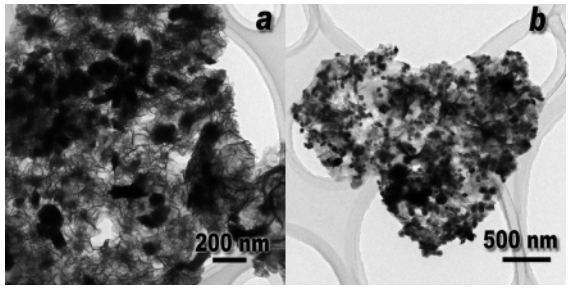

Figure 7. TEM images of the sample prepared at 90 °C over (a) 3 h and (b) 4 h.

anisotropic hindrance role. Second is the subsequent particle crystallization and growth by atom diffusion guided by the concentration gradient of Bi atoms constrained in the film. Naturally, the anisotropic atom diffusion and interparticle aggregation lead to the layered crystalline rhombuses.

Structure-Controlling Solventless Method. We present here some new experimental facts to illustrate our structure-controlling solventless method for converting layered precursors to the layered products. Compared with our previous report on Ag nanodisks,[6] the thermolysis temperature for Bi is remarkably lower than for Ag nanodisks, 90 °C vs 180 °C, a logical difference in itself. This makes it possible for us to isolate a kinetic intermediate—a bismuth nanofilm—to further support the proposed layered-precursor to layered-product conversion mechanism. The observation of the nanofilm might originate with the lower thermolysis temperature. The significance of the as-synthesized film lies in its demonstration that the distribution of the Bi atoms first formed really inherits the layered pattern of the crystal structure of the precursor as we speculated. Furthermore, the in situ film not only serves as the source of bismuth but also restricts its aggregation and diffusion during the subsequent crystallization and growth stages of the to-be-formed rhombuses. These experiment facts further establish that our structure-controlling solventless method is a useful bridge between the crystal structure and the nanoproducts.[16]

Conclusions

In summary, we have successfully synthesized the novel bismuth nanofilms and layered nanorhombuses from the layered bismuth thiolate precursor. The Bi nanofilms are found to be an intermediate between the precursor crystal structure and the layered nanorhombuses. Both the Bi films and the rhombuses are produced on a gram scale with average thicknesses of 0.6 and 0.9 nm, respectively. Interestingly, in the UV−vis range, the rhombuses show an usual 274 nm absorption; the film has two maxima at 257 and 362 nm, and the former peak is a known absorption for Bi nanoparticles while the latter one is new. Some extensions to O- and N-containing ligands and to other binary/ternary alloys and compounds are ongoing, and other possible structural motifs for the conversion are under exploration.

(16) Meyer, G.; Naumann, D.; Wesemann, L. *Inorganic Chemistry in Focus III;* WILEY−VCH: Weinheim, Germany, 2006; Chapter 20, pp 295−303.

Acknowledgment. This research was supported by the National Natural Science Foundation of China under Project Nos. 20401014, 20401013, and 20521101, by the State Key Laboratory Science Foundation (050086 and 050097), NSF of Fujian Province (2004J042, 2005HZ01-1, and 2006J0271), and a ''One Hundred Talent Project" from CAS.

Supporting Information Available: Interlayer spacings, XRD patterns, EDX analyses, particle size distribution, thickness distribution, particle height distribution, and TEM images. This material is available free of charge via the Internet at http://pubs.acs.org.

IC0615067